ARR Oct. 1942

NATIONAL ADVISORY COMMITTEE FOR AERONAUTICS

WARTIME REPORT

ORIGINALLY ISSUED
October 1942 as
Advance [redacted] Report

WIND-TUNNEL INVESTIGATION OF A PLAIN AILERON WITH VARIOUS TRAILING-EDGE MODIFICATIONS ON A TAPERED WING

II - AILERONS WITH THICKENED AND BEVELED TRAILING EDGES

By F. M. Rogallo and Paul E. Purser

Langley Memorial Aeronautical Laboratory
Langley Field, Va.

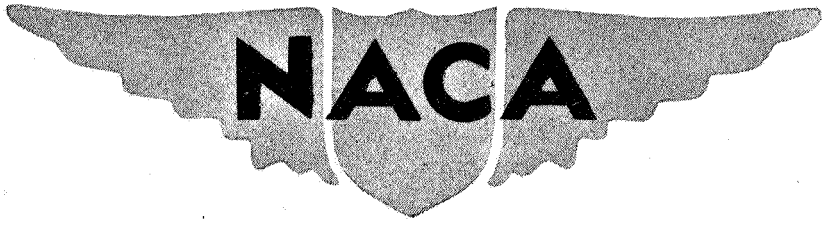

WASHINGTON

NATIGWAL ADVISORY COMMITTEE **FOR** AERONAUTICS

ADVANCE [redacted] REP**OBT**

WIND-TUNNEL INVESTIGATION OF A PLAIN AILERON WITH VARIOUS TRAILING-EDGE MODIFICATIONS ON A TAPERED WING

PI - AILERONS WITH THICKENED AND BEVELED TRAILING EDGES

By F. M. Rogallo and Paul E. Purser

SUMMARY

An investigation was made **in** the LMAL 7- **by** 10-foot tunnel of various modifications to the trailing edge of a 0.155-chord plain aileron on a semispan model of the tapered wing of a fighter airplane. The modifications considered **in** the present report **are** various amounts of thickening and beveling of the aileron trailing edge **to** reduce stick force. The effect of a gap at the aileron nose was determined for the most promising modifications,

The stick forces and the rates of roll were estimated **for** a fighter airplane with the **plain** and with some of the modified ailerons.

The results of the tests and computations indicated that for the arrangement tested the use of beveled **ailerons** would reduce the high-speed stick forces to 60 percent **or** less of those experienced in the use of plain sealed ailerons and would tend to increase the effective dihedral and the damping in **roll,** with the stick free, The **use** of small amounts of thickening and 'beveling of the trailing edge also appears feasible to supplement the action of other types of balance in ***a*** final adjustment of stick forces. Although **not** directly comparable, the results of **the** computations **are** in qualitative agreement with unpublished results of flight tests of an airplane equipped with beveled ailerons. The ill effects of a **gap** at the aileron nose increased as the thickness of the beveled aileron was increased and as the chord of the bevel was decreased,

INTRODUCTION

In view of the increased importance of obtaining adequate lateral control with reasonable stick forces under all flight conditions for high-speed airplanes, tbe NACA hss engaged in an extensive program of lateral-control research. The purposes of this program are to determine the characteristics of existing lateral-control devices, to determine the effects of various modifications to existing devices, and to develop new devices that show promise of being more satisfactory than those now in use. The present tests were made to determine the effects of various amounts of trailing-edge thickening and beveling on the characteristics of a plain aileron, A theoretical discussion and some section data on similar modifications to a symmetrical airfoil and flap have been presented in reference 1,

APPARATUS AND METHODS

Test Installation

A semispan-wing model was suspended in the, LMAL 7- by 10-foot tunnel (reference 2) as shown schematically in figure 1, The root chord of the model was adjacent to one of the vertical walls of the tunnel, the vertical wall thereby serving as a reflection plane. The flow over a semispan in this set-up is essentially the same as it would be over a complete wing in a 7- by 20-foot tunnel. Although a very small clearance was msintained between the root chord of the model and the tunnel wall, no part of the model was fastened to or in contact with the tunnel wall, The model was suspended entirely from the balance frame, as shown in figure 1, in such a way that all the forces and moments acting on it might be determined. Provision'was made for changing the angle of attack while the tunnel, was in operation.

The ailerons were deflected by means of a calibrated torque rod connecting the outboard end of the aileron. with a crank outside the tunnel wall and the hinge moments were determined from the twist of the rod (Pig. 1).

Models

The tapered-wing model used in these tests and In the tests of reference 3 was built to the plan form shown in figure 2 and represents the cross-hatched portion of the airplane shown in figure 3. The basic airfoil sections were of the NACA 230 series tapering in thickness from approximately 15½ percent at the root to 8¼ percent at the tip. The basic chord of the wing was increased 0.3 inch at every spanwise station to reduce the trailing-edge thickness and the last few stations were refaired to give a smooth contour. Ordinates for the extended and refaired sections are given in table I. The details of the ailerons are shown in figure 4. The aileron sections were thickened linearly from the nose arc to the trailing edge and were then beveled symmetrically and linearly to the trailing-edge thickness of the plain, aileron, The beveled portion of the aileron will hereinafter be referred to as the "bevel." The junctures between the ailerons and the bevels were left sharp for some tests and were rounded by arcs of various radii for other tests.

Test Conditions

All except one of the tests were made at a dynamic pressure of 9.21 pounds per square foot, which corresponds to a velocity of about 60 miles per hour and to a test Reynolds number of about 1,540,000 based on the wing mean aerodynamic chord of 33.66 inches, For comparison one test was made at a dynamic pressure of 16,37 pounds'per square foot, which corresponds to a velocity of about 80 miles per hour and to a test Reynolds number of about 2,050,000. The corresponding effective Reynolds numbers for the two values of dynamic pressure were 2,460,000 and 3,280,000 based on a turbulence factor of 1.6 for the LMAL 7- by 10-foot tunnel, The present tests were made at low scale, low velocity, and high turbulence relative to flight conditions to which the results are applied. The effects of these variables were not determined or estimated,

RESULTS AND DISCUSSION

Coefficients and Corrections

The symbols used in the presentation of results are:

C_L lift coefficient (L/qS)

C_D uncorrected drag c'oefficient (D/qS)

C_m pitching-moment coefficient (M/qSc')

$C_{l'}$ rolling-moment coefficient (L'/qbS)

$C_{n'}$ yawing-moment coefficient (N'/qbS)

C_h aileron hinge-moment coefficient $(H/qb_a\overline{c}_a^2)$

ΔC_h C_h of up aileron - C_h of **down** aileron

c actual wing chord at any spanwise location

c_l chord of basic airfoil section at any spanwise location

c' mean aerodynamic chord

c_a aileron chord measured along airfoil. chord line from hinge axis of **aileron** to trailing edge of aileron

$\overline{c}_a$ root-mean-square chord of aileron

c_b chord of beveled portion of aileron trailing edge

R_b radius of Junctura between bevel **and** aileron

At increase in aileron trailing-edge thickness before beveling

b twice **span** of semispan model

b_a aileron **span**

S twice area of semispan **model**

L twice lift on semispan model

D twice drag on semispan **model**

M twice pitching moment **of** semispan model **about support** axis

L' rolling moment, due to aileron deflection, about wind axis in plane of symmetry

N' yawing moment, due to aileron deflection, about wind axis in plane of symmetry'

H aileron hinge moment

q dynamic pressure of air stream uncorrected for blocking $\left(\frac{1}{2}\rho V^2\right)$

V free-stream velocity

V_i indicated velocity

α angle of attack

δ_a aileron deflection from neutral, Chat is, trailing edge on airfoil chord line; positive when trailing edge is down

θ_s control-stick deflection

$C_{l'_p}$ rate of change of rolling-moment coefficient $C_{l'}$ with helix angle $pb/2V$

p rate of roll.

F_s stick force

A positive value of L' or $C_{l'}$ corresponds to an increase in lift of the model, and a positive value of N' or $C_{n'}$ corresponds to a decrease in drag of the model. Twice the actual lift, drag, pitching moment, area, and span of the model were used in the reduction of the results because the model represented half a complete wing, The drag coefficient and the angle of attack have been corrected only in accordance with the theory of trailing-vortex images. 'Corresponding corrections were applied to the rolling-'and yawing-moment coefficients, No correction has been applied Lo the hinge-moment coefficients. No corrections have been applied to' any of the results for blocking, for the effects of the support strut, or for the treatment of the inboard end of the wing,' Chat is, the small gap between the wing and the wall,' the leakage, through the wall around the support tube, and the 'boundary layer at the wall. These effeots

are probably of second-order importance for the rolling- and yawing-moment coefficients (which are basically incremental data) but may have more effect on the other forces and moments, particularly on the drag coefficients. It is for this reason that the drag coefficients are referred to as uncorrected,

Characteristics with Ailerons Neutral

The characteristics of the wing model with the various ailerons fixed at zero deflection are shown in figure 5. The beveled trailing edges reduced the slope of the wing lift curve $\partial C_L/\partial \alpha$ from 0.076 to 0.070 per degree, reduced the maximum lift coefficient from 1.36 to 1.34, and increased the minimum drag coefficient from about 0.0110 to abont 0,0115. The effect of the beveled trailing edges on the slope of the pitching-moment curve $\partial C_m/\partial C_L$ increased with bevel thickness; the thicker bevel changed the slope by about 0.01 which corresponds to a forward shift of about $0.01c'$ in the aerodynamic center of the wing,

The effects of the beveled, trailing edges on the characteristics of the model with ailerons neutral are in qualitative agreement with the effects reported in reference 1,

Aileron Characteristics

Plain ailerons.- The characteristics of the plain sealed and unsealed ailerons are presented in figure 6. A comparison of the increments between $\delta_a = 15^\circ$ and $\delta_a = -15^\circ$ shows that the presence of a $0.005c$ gap at the aileron nose reduced the rolling-moment coefficient by about 16 percent and increased the hinge-moment coefficient by about 12 percent; the gaps had little effect on the slope of the hfnge-moment curve $\partial C_h/\partial \delta_a$ at small deflections.

Beveled ailerons.- The characteristics of the various beveled ailerons are presented in figures 7 to 17, The first of the ailerons to be tested had. a $0.02c$ increase in trailing-edge thickness before beveling and the chord of the bevel was $0.20c_a$; the corners of the bevel were

left sharp and the 0.005c gap at the aileron nose was left open. As shown in figure 7, the aileron vas considerably overbalanced for a deflection range of ±4° near zero angle of attack. The slope of the hinge-moment curve against angle of attack $\partial C_h/\partial \alpha$ was predominantly positive for negative aileron deflections and small positive deflections and was predominantly negative for positive deflections larger than 10°. The positive $\partial C_h/\partial \alpha$ near neutral would tend to increase the effective dihedral and the damping in roll with the stick free but, under the same conditions, would magnify the acceleration in roll due to an asymmetric vertical gust. Figures 8, 9, and 10 show that rounding the corners of the bevel and scaling the gap at the aileron nose eliminated the overbalanced. tendency of the aileron. The effectiveness of the aileron increased as %he gap was reduced and as the bevel radius was increased.

Figure 11 shows the effect of scale on the aileron with the sealed gap and the thick short, bevel, The increased speed increased the balancing-tab action of the bevel as indicated by the reduction in both the hinge-moment and rolling-moment coefficients due to aileron deflection,

An increase in the bevel- chord to an average of $0.34c_a$ decreased the balancing action of the bevel.; part of thie loss in balancing action was restored by building up the trailing edge with wax until it was approximately halfway between the long and the short bevels, (See fig. 12.)

The effects of the bevel radius and the gap at the aileron nose on an 'aileron with an increase in thickness of 0.01c and a bevel, chord of $0.20c_a$ are shown in figures 13, 14, and 15, The overbalancing tendency and the effects of gap and bevel. radius on the overbalancing tendency decreased. with the decrease in bevel thickness. For the aileron with a $0.20c_a$ bevel radius, a reduction in the gap at the aileron nose from 0,0050c to 0.0025c apparently eliminatad the overbalancing tendency, (See fig, 14.) An increase in the bevel length to an average of $0.34c_a$ reduced the balancing action of the bevel so much that no further tests were made on the thin aileron with the long bevel (fig, 16).

Comparative plots showing the effects of bevel chord and thickness on the characteristics of the beveled ailerons are shown in figure 17. An increase in the chord of the bevel or a decrease in its thickness reduced the overbalancing tendency that the ailerons with gaps exhibited at small deflections but also reduced the deflection range over which the slope of the hinge-moment curve $\partial C_h/\partial \delta_a$ was appreciably less than that of the plain aileron. For the ailerons with sealed gaps, the same effects were noted except that the changes at small aileron deflections were less pronounced.

The discrepancies between the check tests and the regular tests shown in figures 9(a) and 14(a) probably resulted from the aileron-wing installation having been completely dismantled and then reassembled, with some parts replaced, between the running of the two series of tests. The first series of tests included all those with sealed and 0.005c gaps and the second series included the sealed-gap check tests and the tests with 0.0025c and 0.0013c gaps.

The tests showed larger effects due to the gap at the aileron nose than those shown by the tests reported in reference 1. The larger gap effects may have been due to the fact that the relative chord of the control surface of the present tests was much smaller than that of the control surface of the tests reported in reference 1.

Estimated Rates of Roll and Stick Forces

The rates of roll and the stick forces during steady rolling of the airplane of figure 3 have been estimated from the data of figures 6, 8, 12, and 15. The rates of roll were estimated by means of the relationship

$$\frac{pb}{2V} = \frac{C_l'}{C_{l'_p}} \qquad (1)$$

where the coefficient of damping in roll $C_{l'_p}$ was taken, for the wing with plain ailerons, as 0.46 from the data of reference 4. For the beveled ailerons, the value of $C_{l'_p}$ was reduced to 0.425 because of the decrease in the

slope of the wing lift curve due to the beveled trailing edge. (See fig. 5.) It has been assumed that the rudder will be used to counteract the yawing moment and wing twist has been neglected. The stick forces were estimated from the relationship

$$F_s = \frac{20.3}{C_L} \Delta C_h \frac{dS}{d\theta_s} \qquad (2)$$

which may be derived from the aileron dimensions and the following airplane characteristics:

Wing area, square feet	260
Span, feet	38
Paper ratio	1.67:1
Airfoil section (basic)	NACA 230 series
Mean aerodynamic chord, inches	84.14
Weight, pounds	7063
Wing loading, pounds per square foot	27.2
Stick length, feet	2
Maximum stick deflection, θ_s, degrees	±21

The value of the constant in equation (2) is dependent upon the wing loading, the size of the ailerons, and the length of the stick. The values of $d\delta_a/d\theta_s$ in equation (2) may be determined from the maximum stick deflection of $\pm 21^\circ$ and from the masimum aileron deflections noted on the figures of computed results; $d\delta_a/d\theta_s$ is assumed constant. The values of C_l' and ΔC_h used in equations (1) and (2) are the values thought to exist during steady rolling; the difference in angle of attack of the two ailerons due to rolling has been taken into account.

The results of the computations (fig. 18) indicated that the use of a beveled trailing edge would reduce the high-speed stick forces to approximately 60 percent of those obtained from plain sealed ailerons for the same rolling effectiveness. These results, though not directly comparable, are in general agreement with unpublished results of flight testa of an airplane equipped with beveled ailerons,

The effect of steady rolling on the high-speed stick forces is shown in figure 19 for the plain aileron and for one of the 'beveled ailerons. Rolling reduced the

maximum high-speed stick force by about 6 pounds for the plain ailerons **because** of the negative value of $\partial C_h/\partial \alpha$. For the beveled aileron, the value of $\partial C_h/\partial \alpha$ **was** positive at the high-speed attitude, and rolling therefore increased the maximum high-speed stick force by about 2 pounds. The increase in stick **force** at low deflections **due** to rolling **was** enough to eliminate the overbalance in the stick-force curve that was computed for the static state.

The positive value of $\partial C_h/\partial \alpha$ for the beveled aileron, moreover, increases the effective dihedral and the damping in **roll** with the **stick** free; whereas with the plain aileron the negative value of $\partial C_h/\partial \alpha$ has the **Opposite** effect, Although the beveled ailerons would be expected to cause a more rapid return. of the airplane to a level attitade after a given displacement in roll, it is likely that they would magnify the effects of an asymmetric vertiaal gust, relative *to* the plain ailerons, the stick being considered free in all cases,

CONCLUSIONS

The results of the tests of 0.155-chord ailerons on an *NACB* 230 **series** airfoil **and** the computations indicated that for the arrangement tested the use of beveled ailerons would reduce the high-speed stick forces to 60 percent or less of those esperienced in the use of plain sealed ailerons and would increase the effective dihedral and the damping in **roll** with the **stick** free. The use of small amounts of thickening and beveling of the trailing edge also appears feasible to supplement the action of other types of balance in a final adjustment **of** stick forces. The results 'of the computations, though **not** directly comparable, are in general agreement with unpublished results of flight tests of an airplane equipped with beveled ailerons. The **ill** effects of a gap at the aileron nose. increased as the thickness of **the** beveled aileron was increased and as the chord of the bevel was decreased.

Langley Memorial Aeronautical Laboratory,
National **Advisory** Committee for Aeronautics,
Langley Field, Va.

REFERENCES

1. Jones, Robert T., and Ames, Milton B., Jr.: Wind-Tunnel Investigation of Control-Surface Characteristics, V - The Use of a Beveled Trailing Edge to Reduce the Hinge Woment of a Control Surface. NACA A.R.R., March 1942.

2. Wenzinger, Carl J., and Harris, Thomas A.: Wind-Tunnel Investigation of an N.A.C.A. 23012 Airfoil with Various Arrangements of Slotted Flaps, Rep, No, 664, NACA, 1939.

3. Rogallo, F. M., and Lowry, John G.: Wind-Tunnel Investigation of a Plain Aileron and a Balanced Aileron on a Tapered Wing with Full-Span Duplex Flaps. NACA A.R.R., July 1942.

4, Gilruth, R. R., and Turner, W. N.: Lateral Control Required for Satisfactory Flying Qualities Based on Flight Tests of Numerous Airplanes, Rep, No. 715, NBCA, 1941.

TABLE I

ORDINATES FOB AIRFOIL

[Spanwise stations in inches from root section, Chord stations and ordinates in percent of 'basic wing chord c_1]

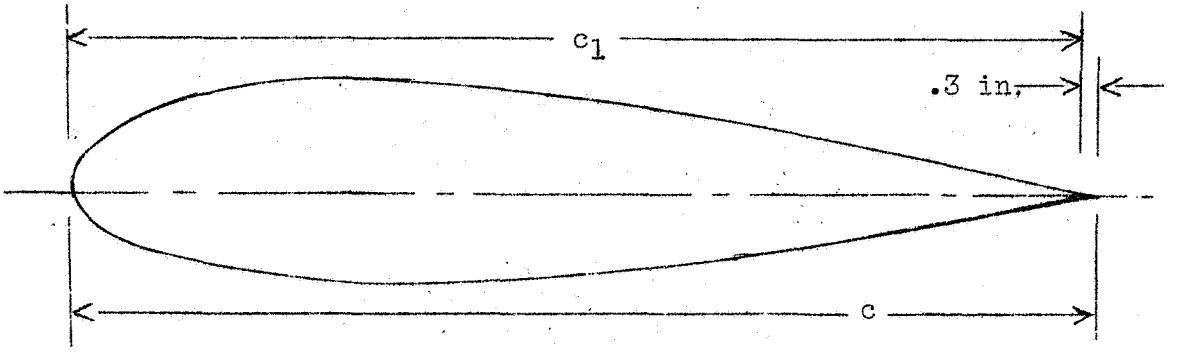

Model wing station 0		
Station	Upper surface	Lower surface
0	0	0
1.25	3.48	-1.60
2.5	4.61	-2.36
5	6.10	-3.21
7.5	7.14	-3.82
10	7.89	-4.33
15	8.80	-5.12
20	9.22	-5.71
25	9.40	-6.10
30	9.37	-6.28
40	8.90	-6.23
50	8.02	-5.78
60	6.85	-5.05
70	5-44	-4.10
80	3.87	-2.97
90	2.12	-1.67
95	1.16	-.94
100	.18	-.16
100.73	.03	-.03
L.E. radius: 2.65. Slope of radius through end of chord; 0,305		

Model wing station 88.8		
Station	Upper surface	Lower surface
0	0	0
1.25	1.89	-.84
2.5	2.65	-1.07
5	3.70	-1.26
7.5	4.45	-1.40
10	4.98	-1.52
15	5.54	-1.86
20	5973	-2.22
25	5777	-2.46
30	5.71	-2.62
40	5.36	-2.70
50	4.78	-2.56
60	4.06	-2.27
70	3.21	-1.87
80	2.26	-1.36
90	1.22	-.78
95	.70	-.46
100	.18	-.14
101.2	.05	-.05
L.E. radius; 0.70. Slope of radius through end of chord: 0,305		

L-228

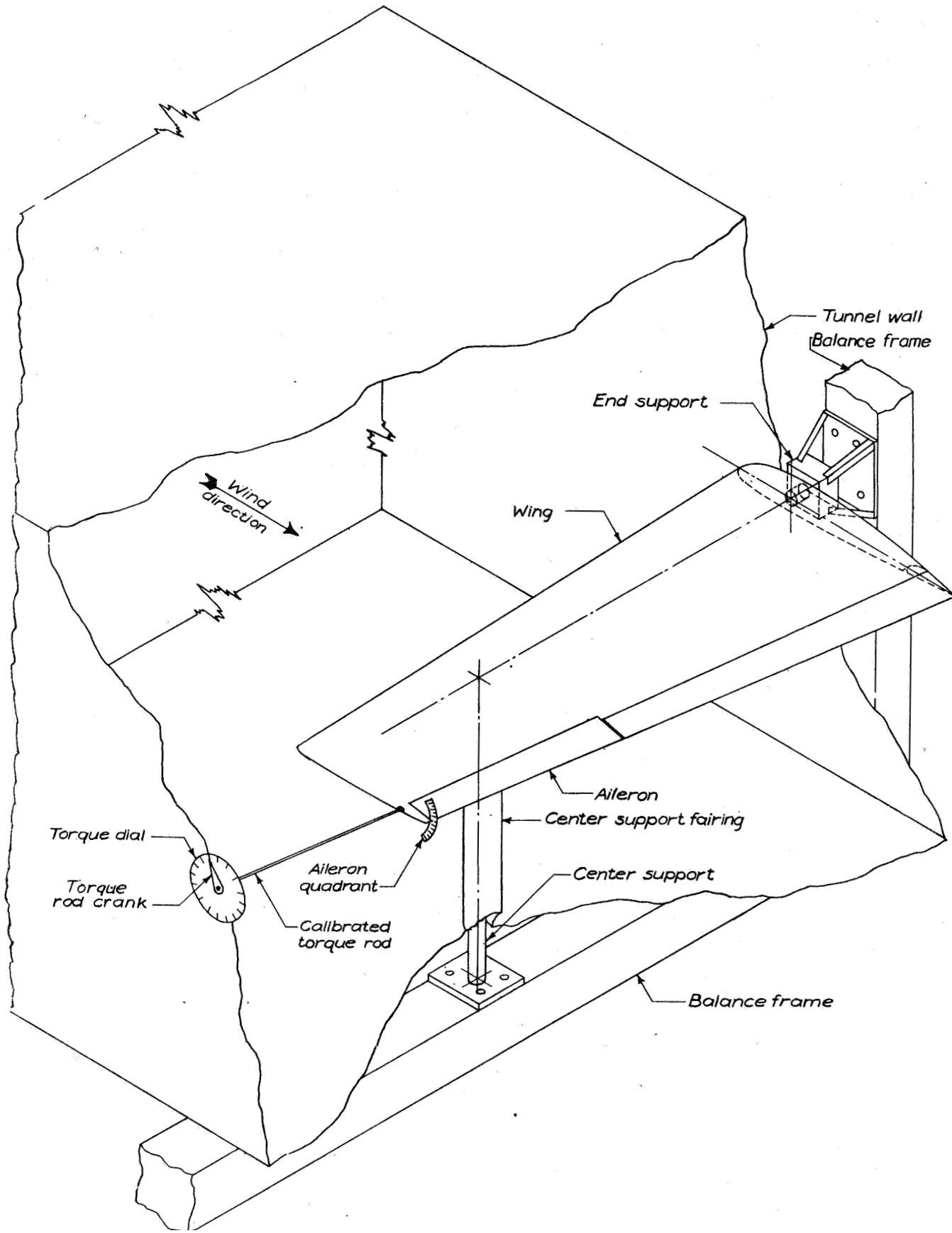

a

Figure 1.- Schematic diagram of test installation.

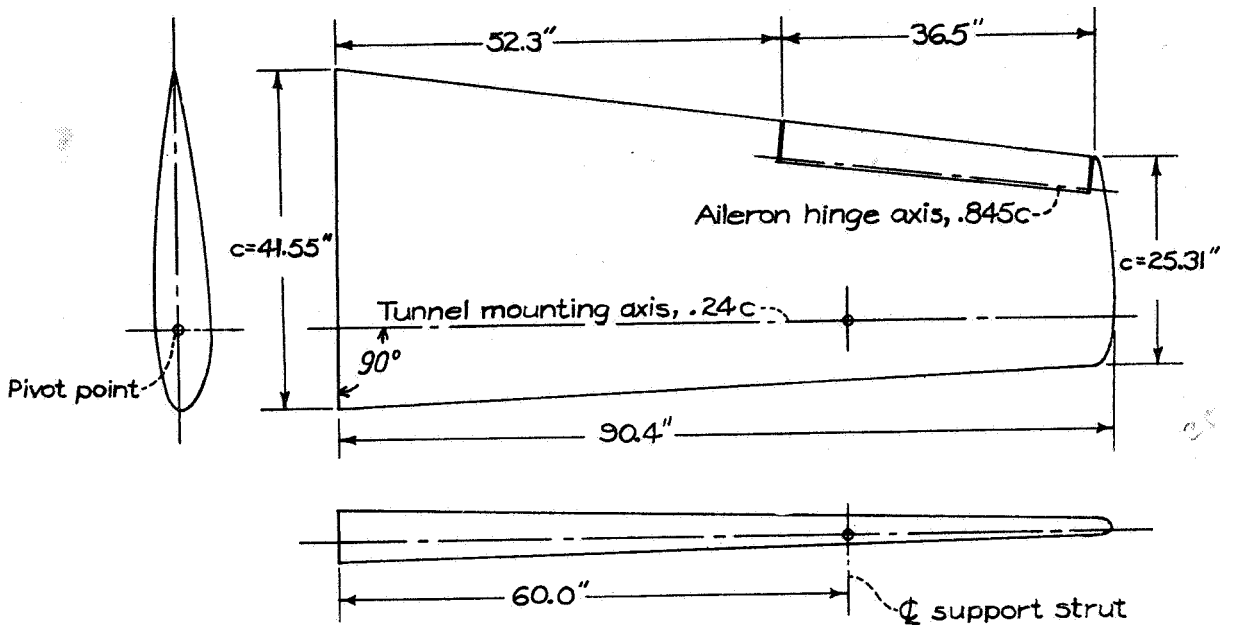

Figure 2.- Semispan model of **tapered** wing.

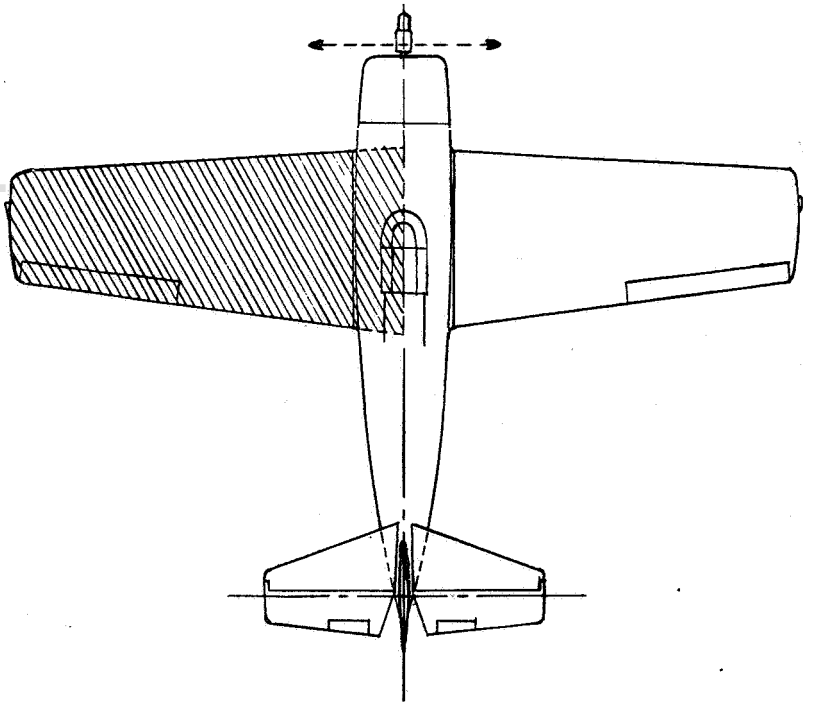

Figure 3.- Portion of airplane simulated by model.

L-228

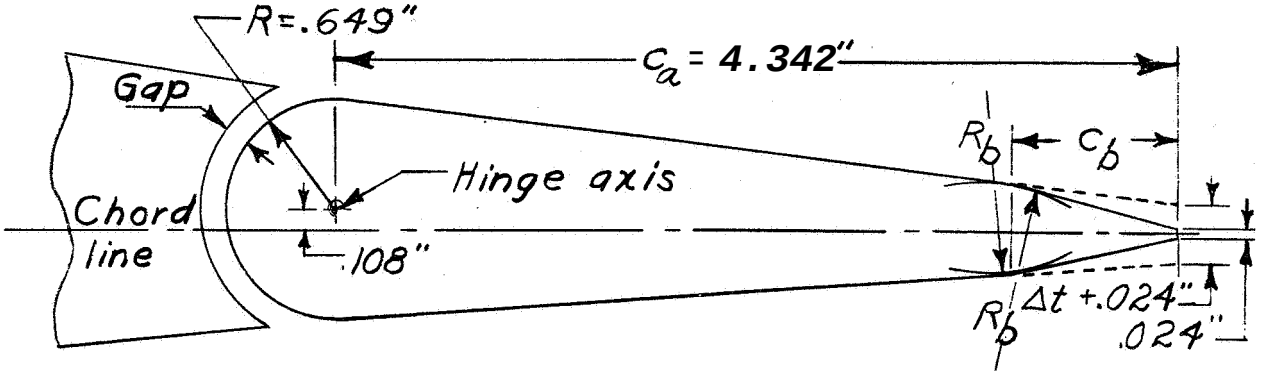

(a) Inboard end; wing chord c = 31.986".

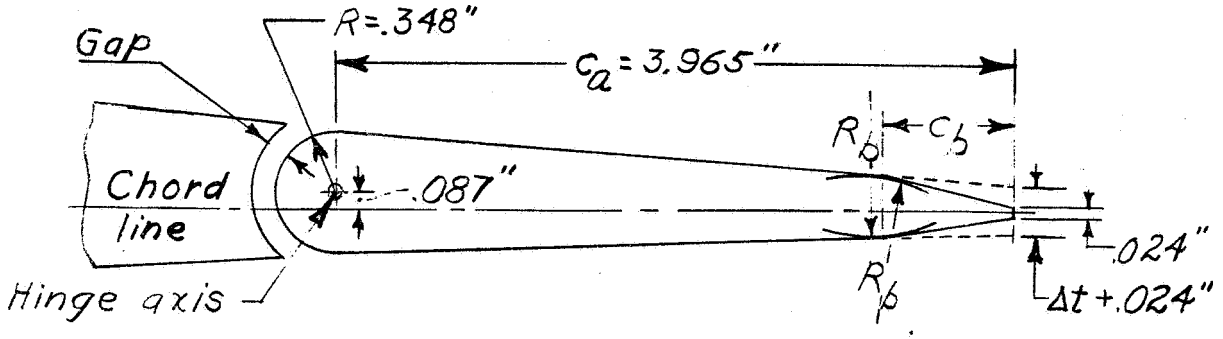

(b) Outboard end; wing chord c = 25.314".

Aileron	Bevel	c_b, percent c_a		Δt, percent c
		Inboard	Outboard	
1	1	20	20	2.0
1	2	32.6	35.5	2.0
2	1	20	20	1.0
2	2	32.6	35.5	1.0

Gap and R_b were varied during tests and are noted on figures that show test results.

Figure 4.- The 0.155c by 0.405 $^b/_2$ beveled ailerons tested on the tapered-wing model.

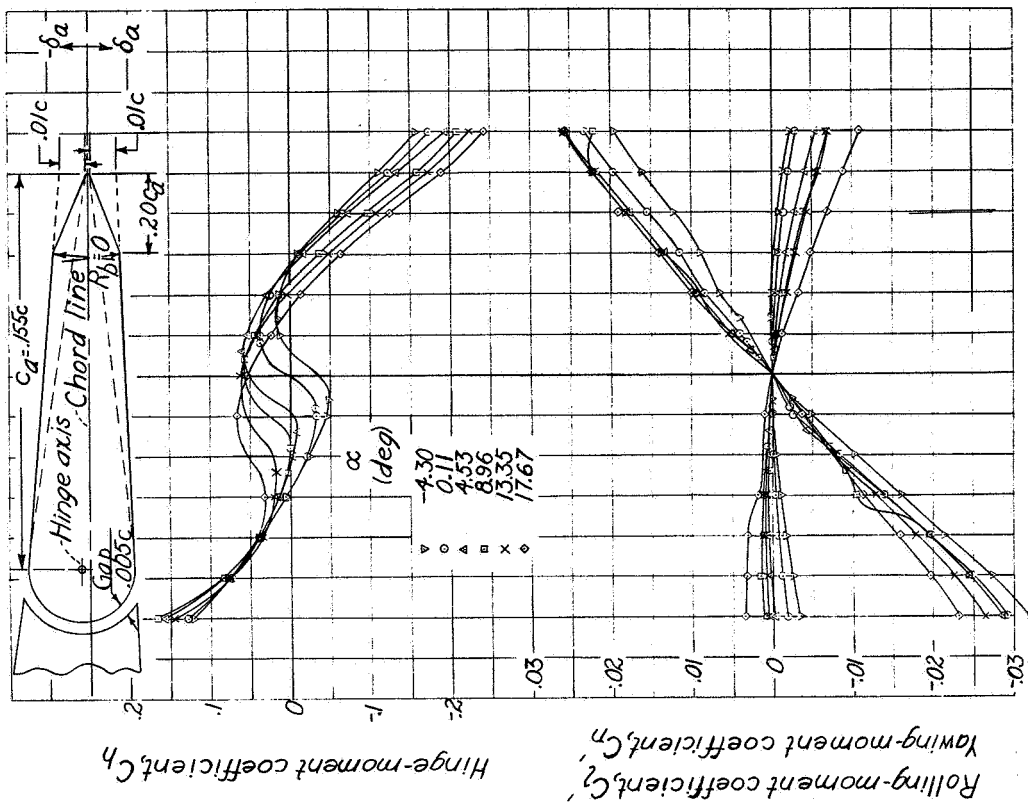

Figure 7.- Characteristics of a beveled aileron on the tapered-wing model. 0.005c gap; c_b, 0.20c_a; Δt, 0.02c; R_b, 0.

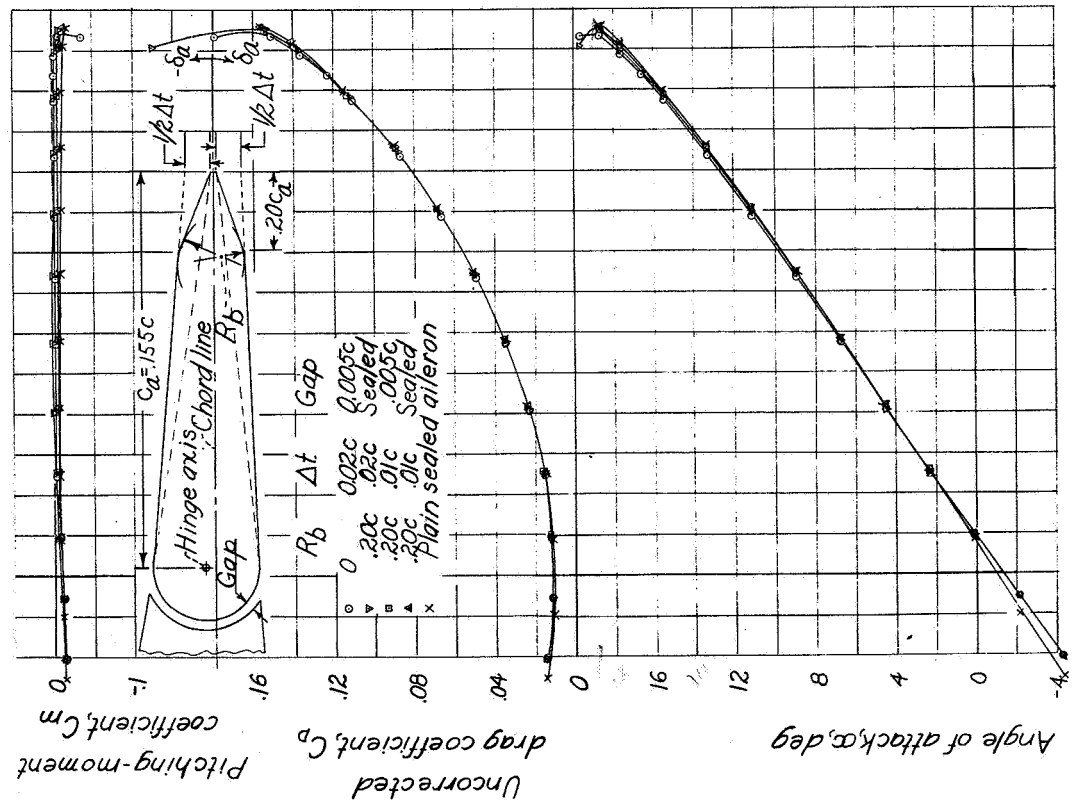

Figure 5.- Characteristics of the tapered-wing model with the various ailerons fixed at zero deflection.

L-228

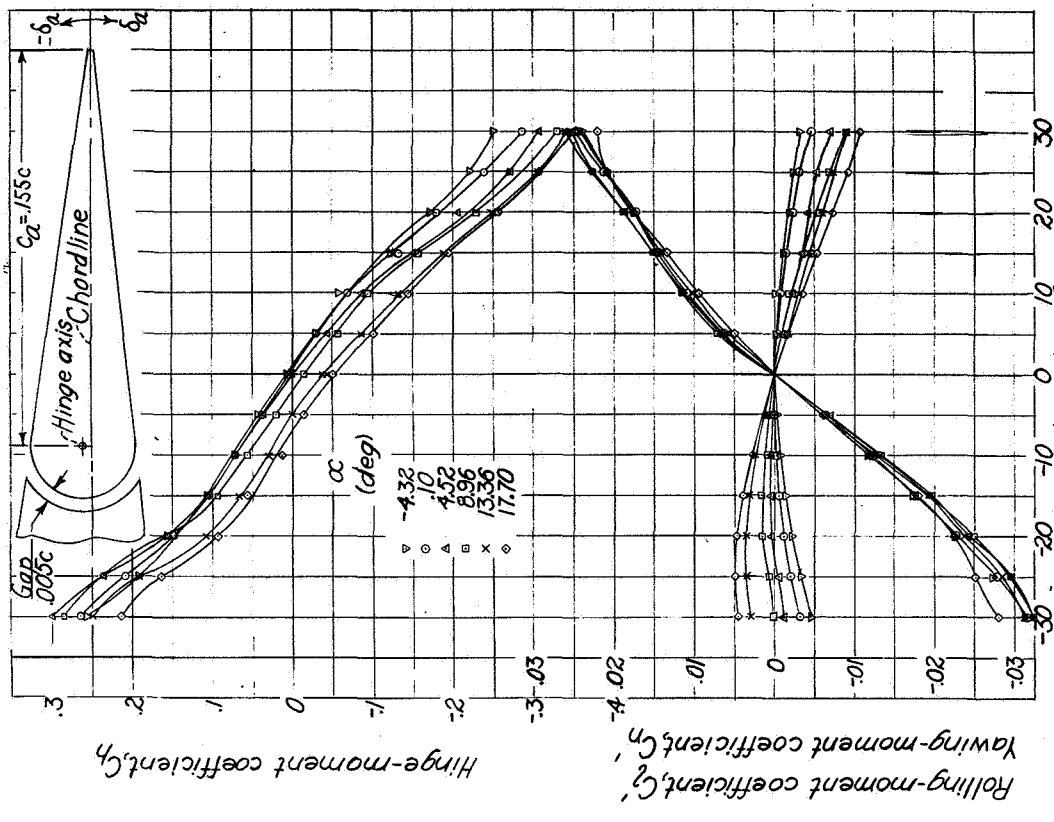

(b) 0.005c gap.

Figure 6.- Concluded.

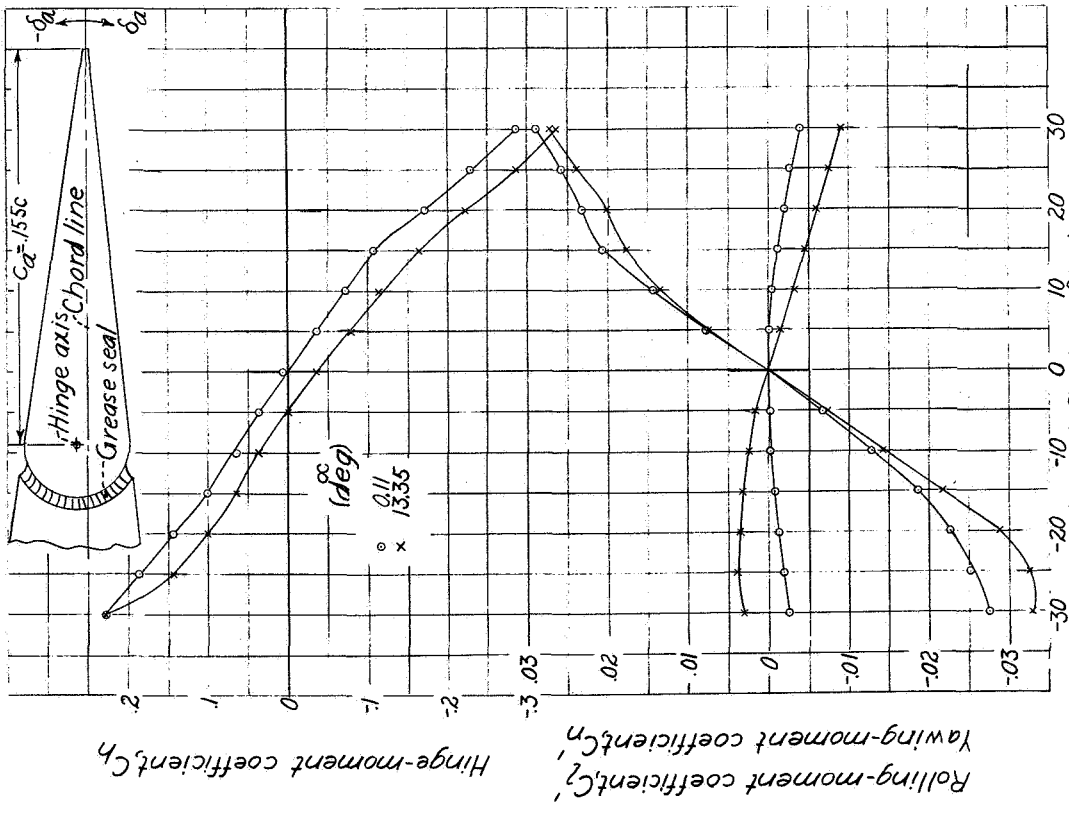

(a) Sealed gap.

Figure 6.- Characteristics of the plain aileron on the tapered-wing model.

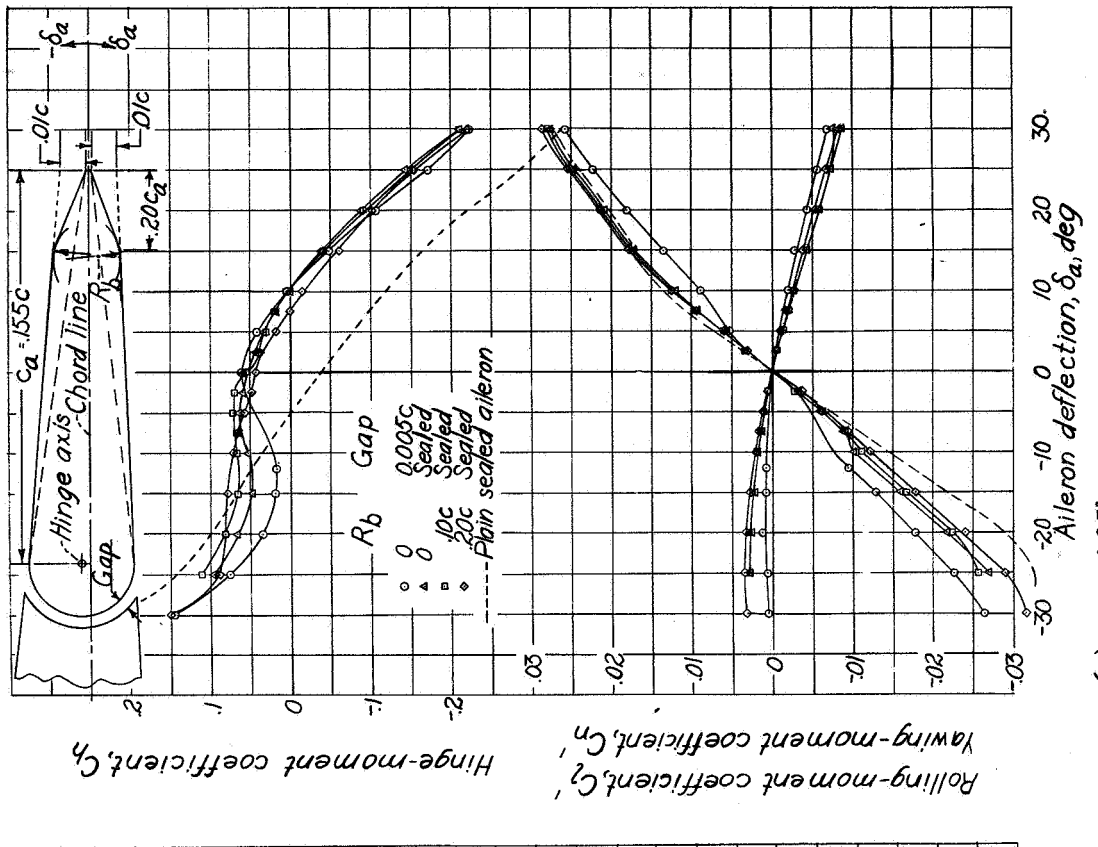

(b) α = 13.3°.

Figure 8.- Concluded.

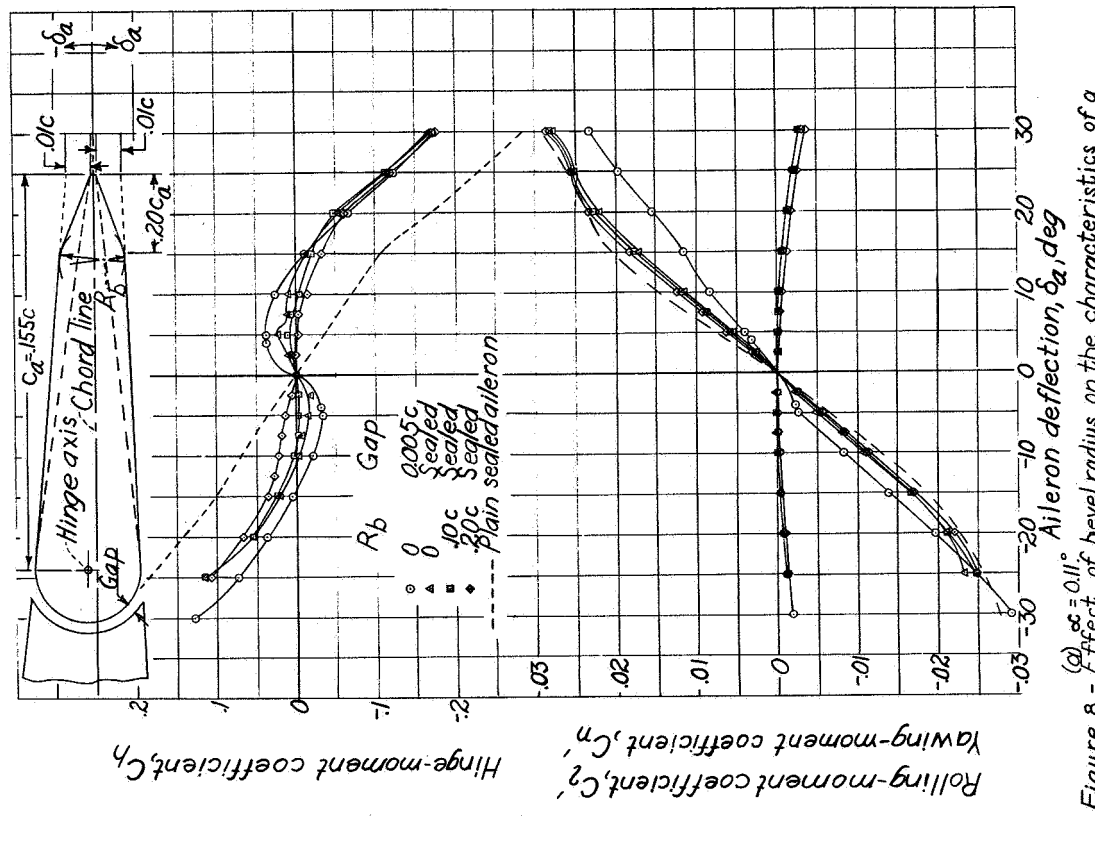

Figure 8.- (a) α = 0.1°. Effect of bevel radius on the characteristics of a beveled aileron on the tapered-wing model. c_b, 0.20 c_a; Δt, 0.02c.

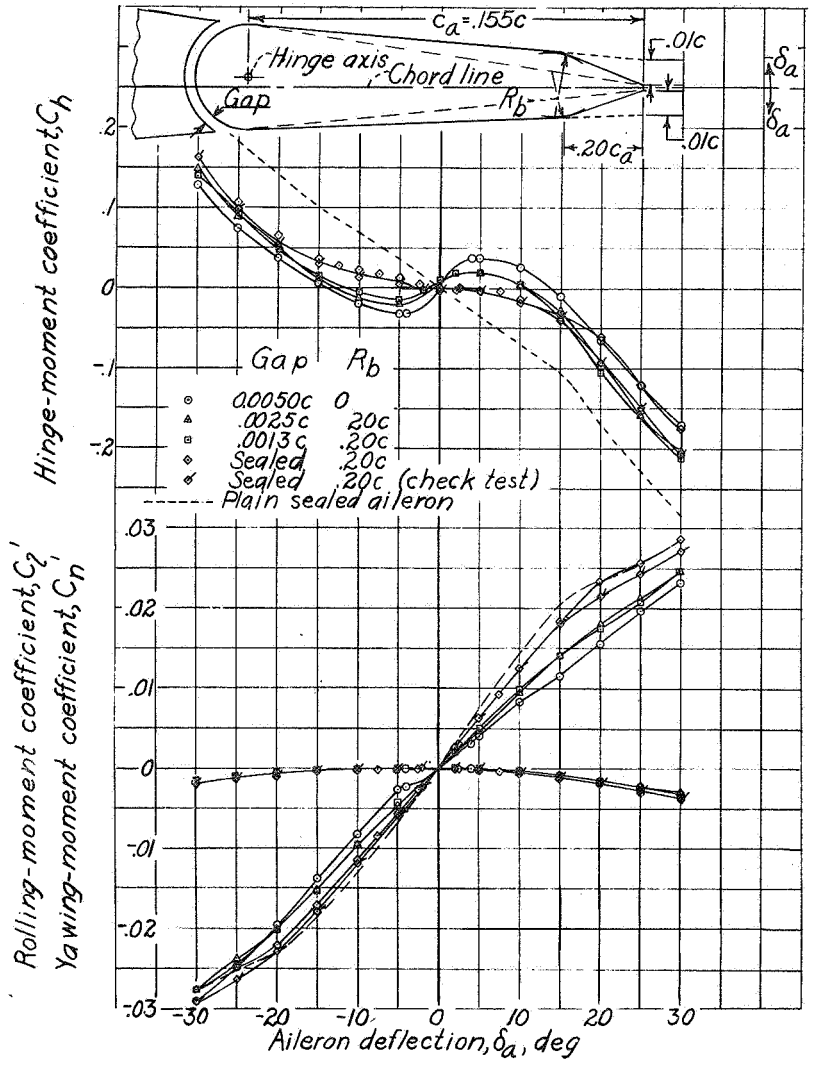

(a) α = 0.11°.

Figure 9.- Effect of gap on the characteristics of a beveled aileron on the tapered-wing model. c_b, 0.20c_a; Δt, 0.02c.

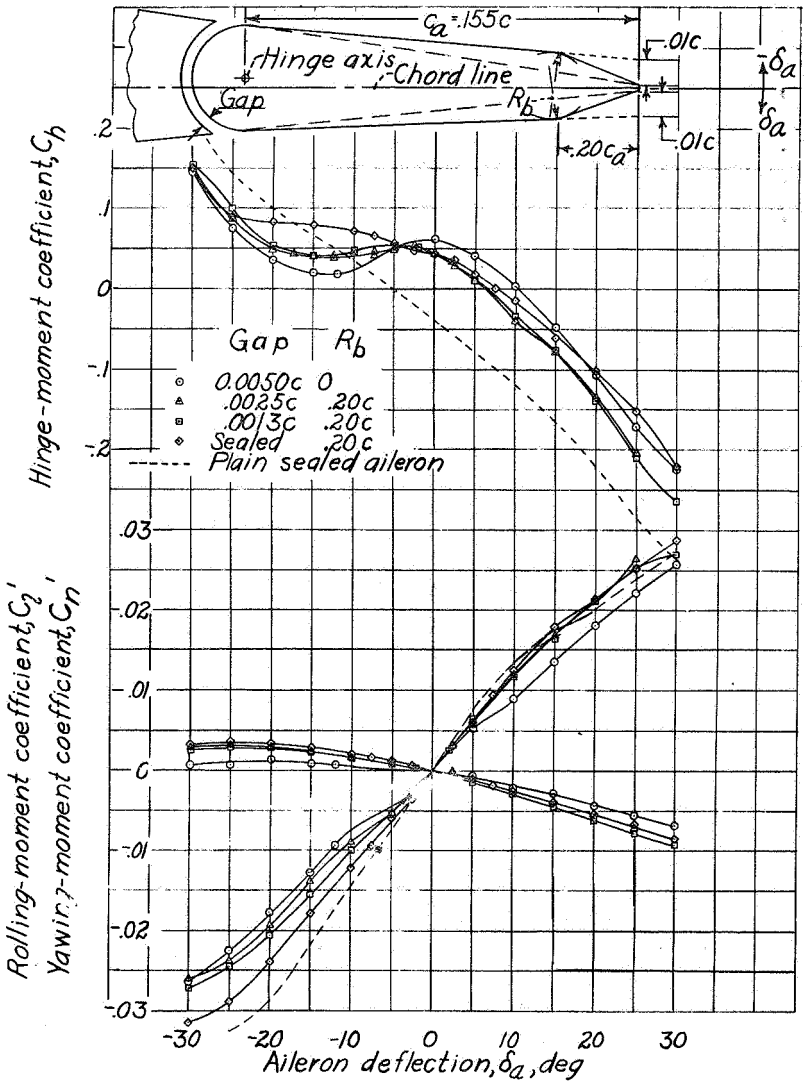

(b) α = 13.35°.

Figure 9.- Concluded.

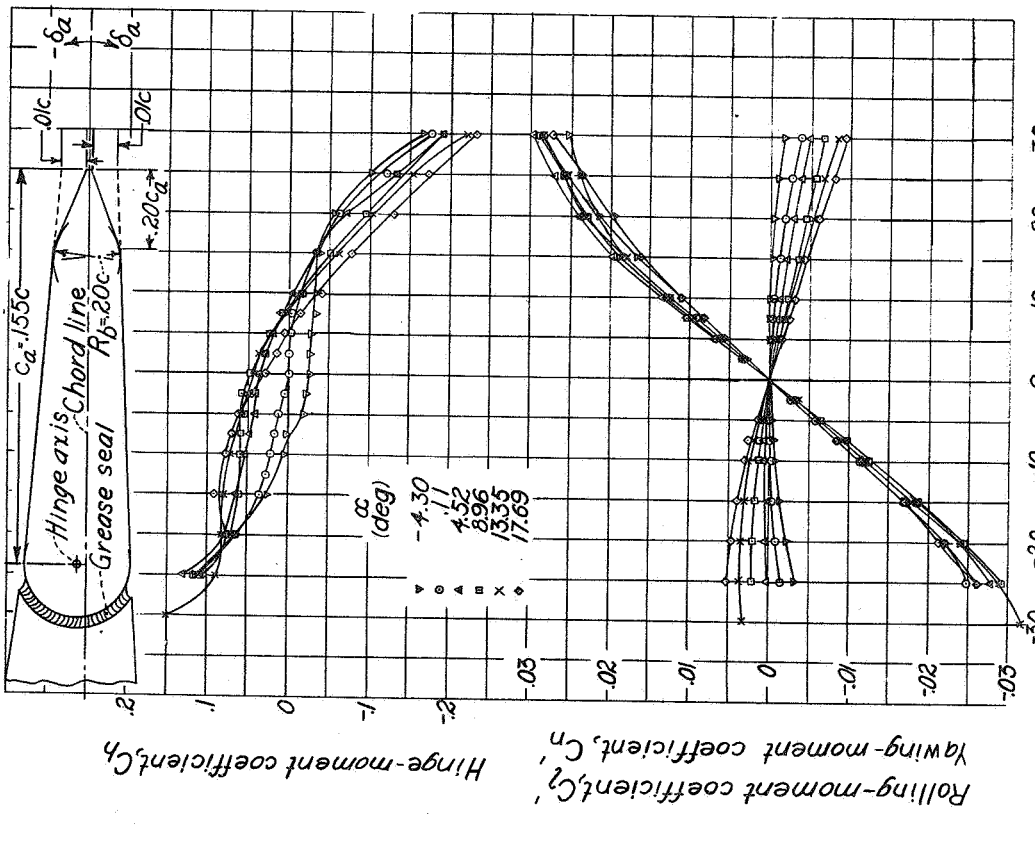

Figure 10.- Characteristics of a beveled aileron on the tapered-wing model. Sealed gap; c_b, 0.20c_a; Δt, 0.02c; R_b, 0.20c.

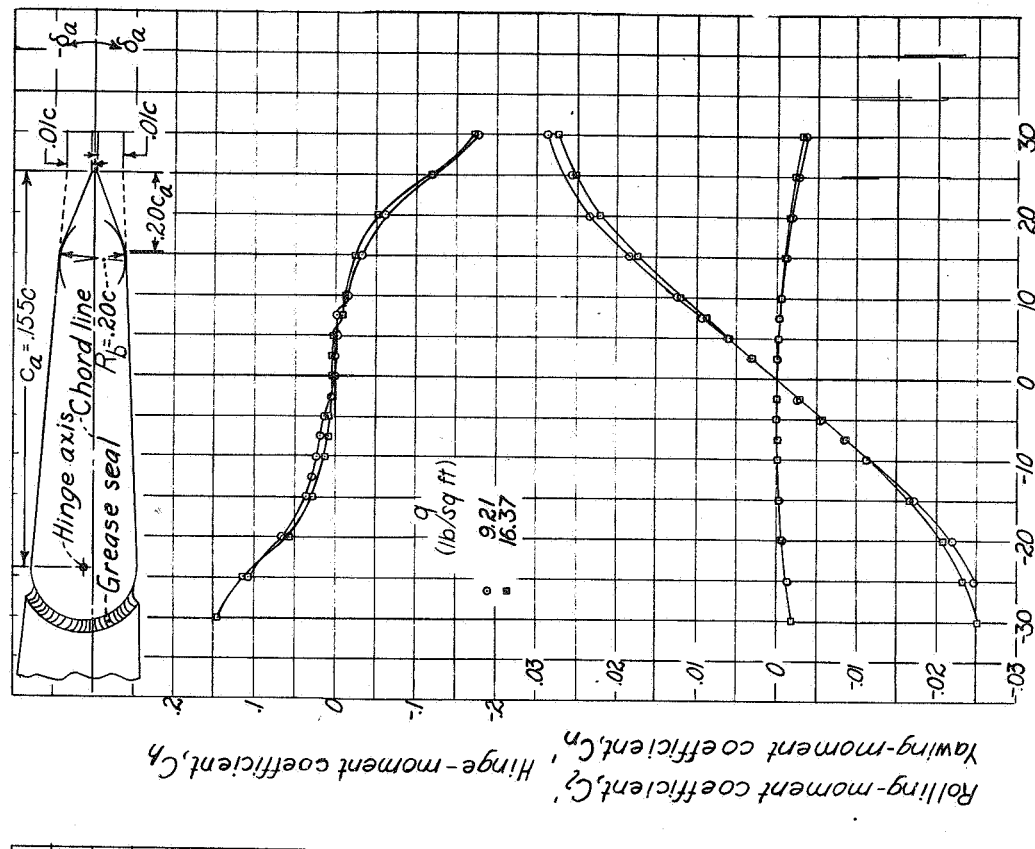

Figure 11.- Effect of scale on the characteristics of a beveled aileron on the tapered-wing model. Sealed gap; c_b, 0.20c_a; Δt, 0.02c; R_b, 0.20c; α, 0.11°.

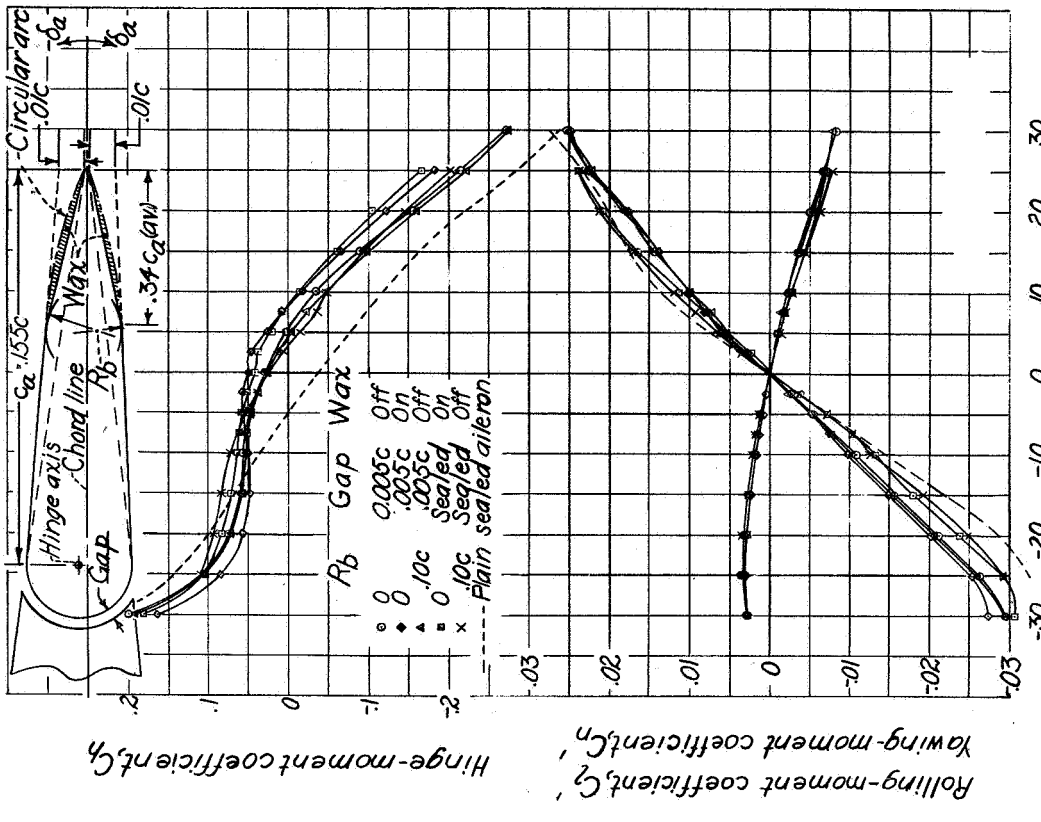

(b) α = 13.35°.

Figure 12.- Concluded.

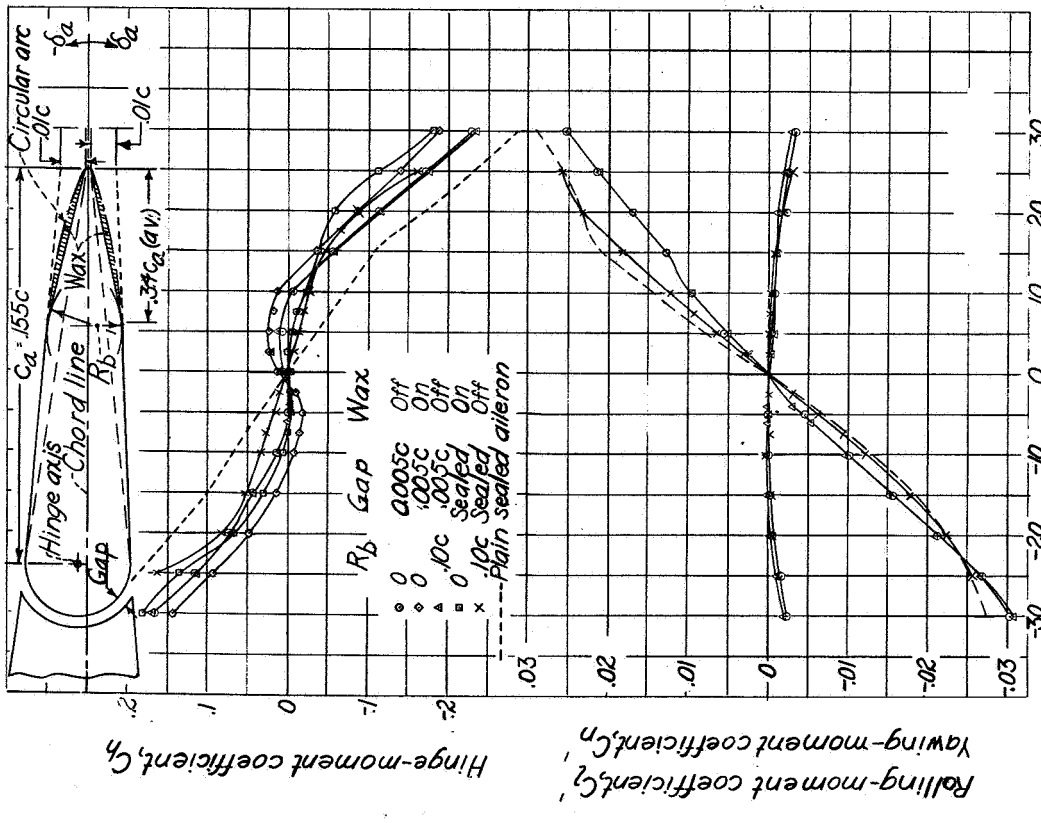

Figure 12.- (a) α = 0.11°. Effect of gap and bevel radius on the characteristics of a beveled aileron on the tapered-wing model. c_b, 0.34c_a ; Δt, 0.02c .

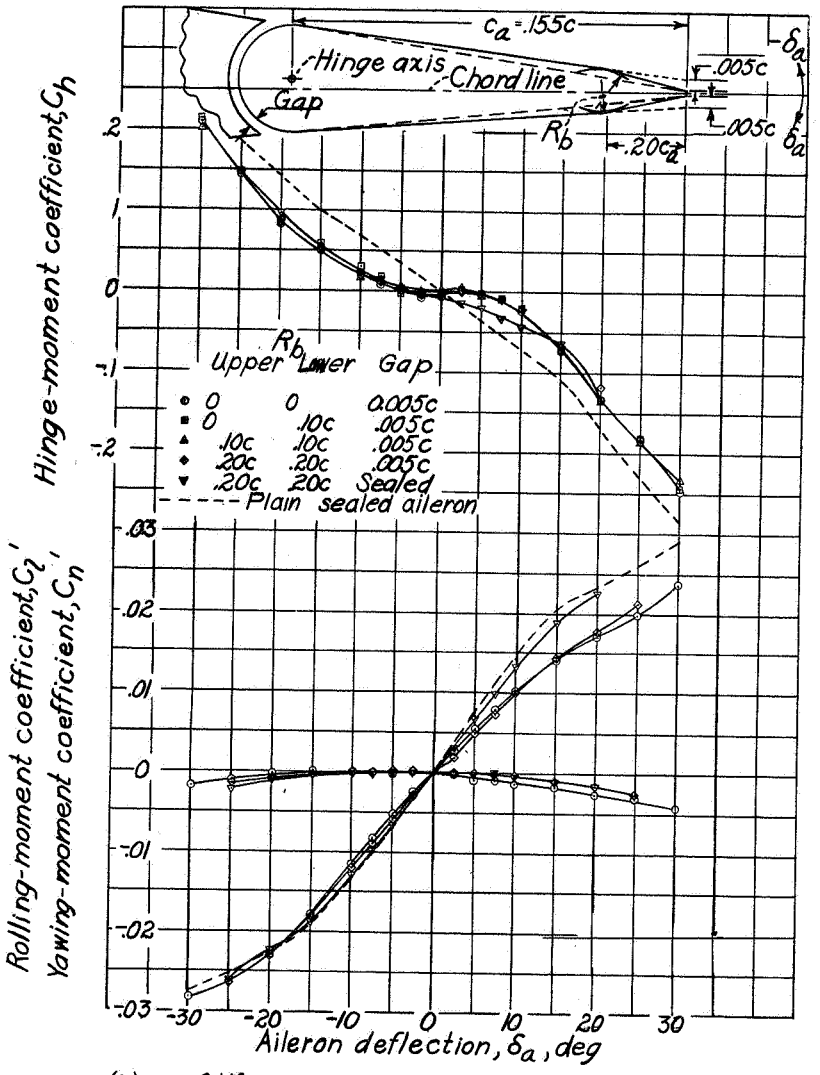

(a) α = 0.11°

Figure 13 - Effect of bevel radius on the characteristics of a beveled aileron on the tapered-wing model. c_b, 0.20 c_a ; Δt, 0.01c.

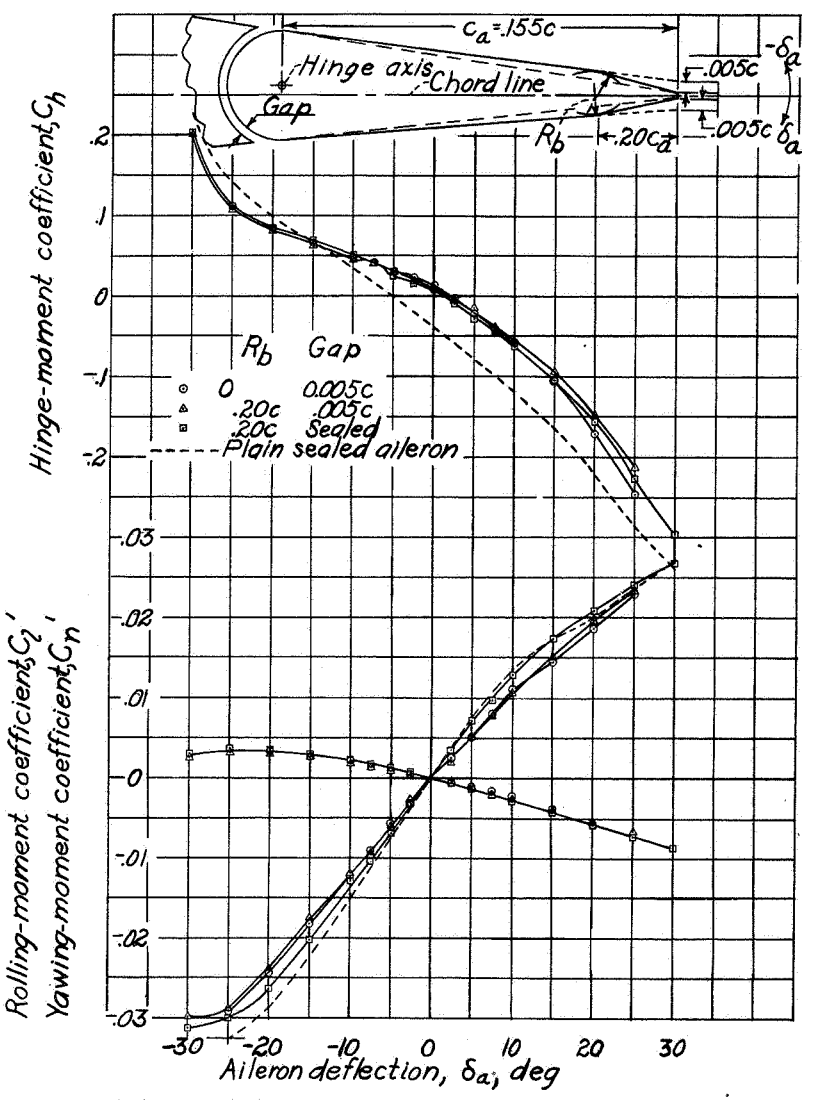

(b) α = 13.35°

Figure 13. - Concluded.

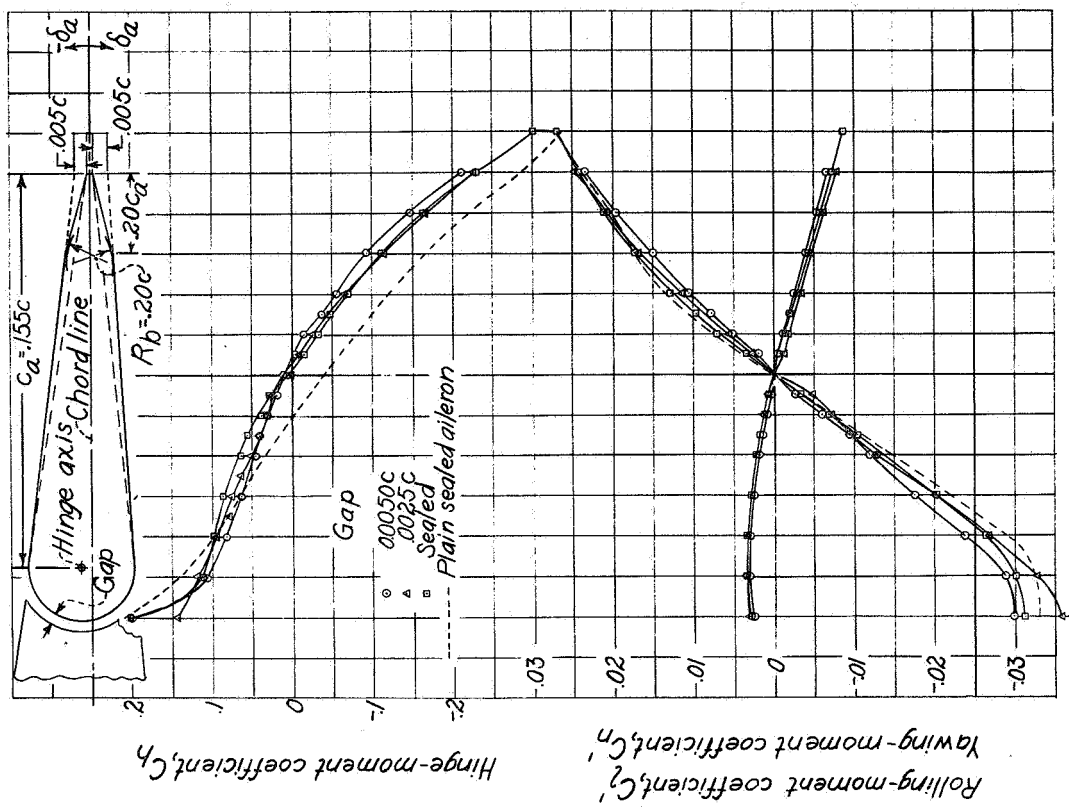

(b) $\alpha = 13.35°$.

Figure 14.- Concluded.

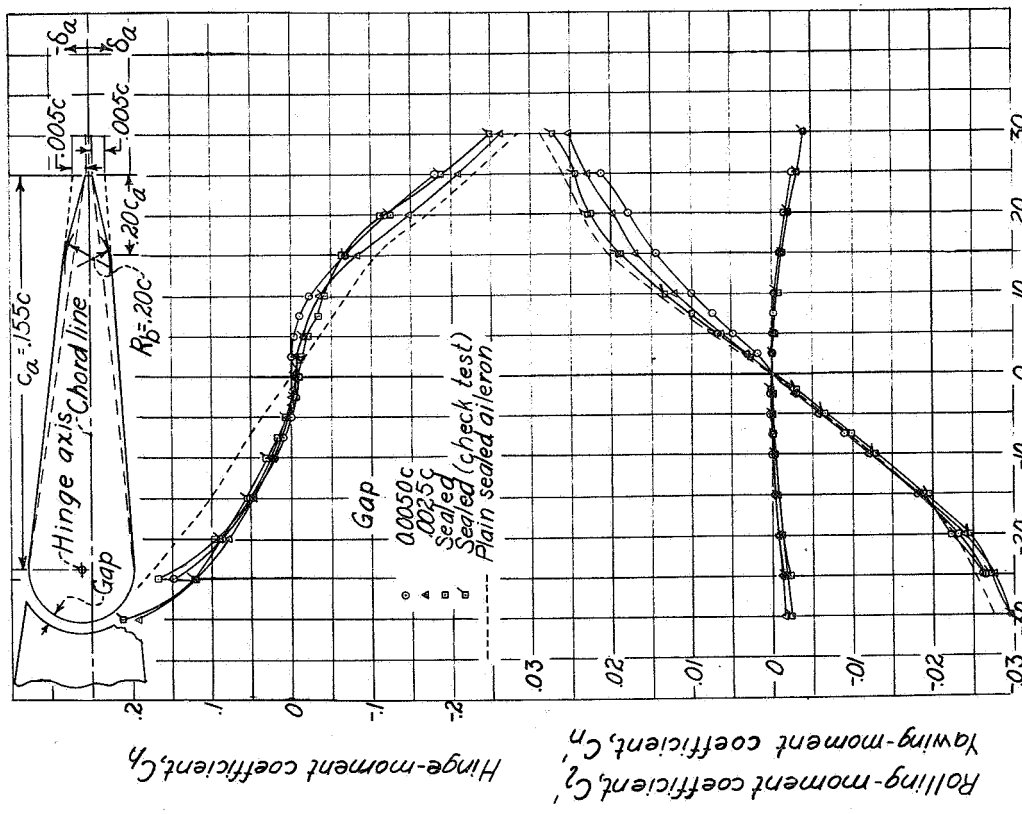

(a) $\alpha = 0.11°$.

Figure 14.- Effect of gap on the characteristics of a beveled aileron on the tapered-wing model. $c_b, 0.20c_a$; $\Delta t, 0.01c$; $R_b, 0.20c$.

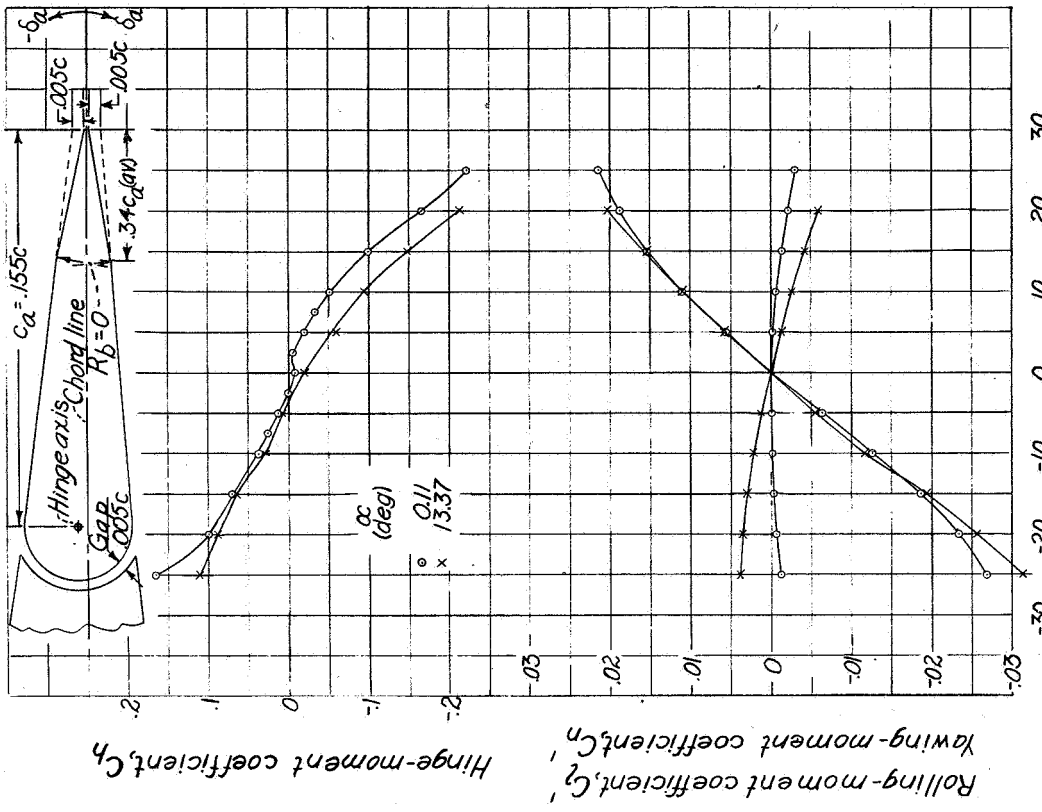

Figure 16.- Characteristics of a beveled aileron on the tapered-wing model. 0.005c gap ; c_b, 0.34c_a ; Δt, 0.01c; R_b, 0

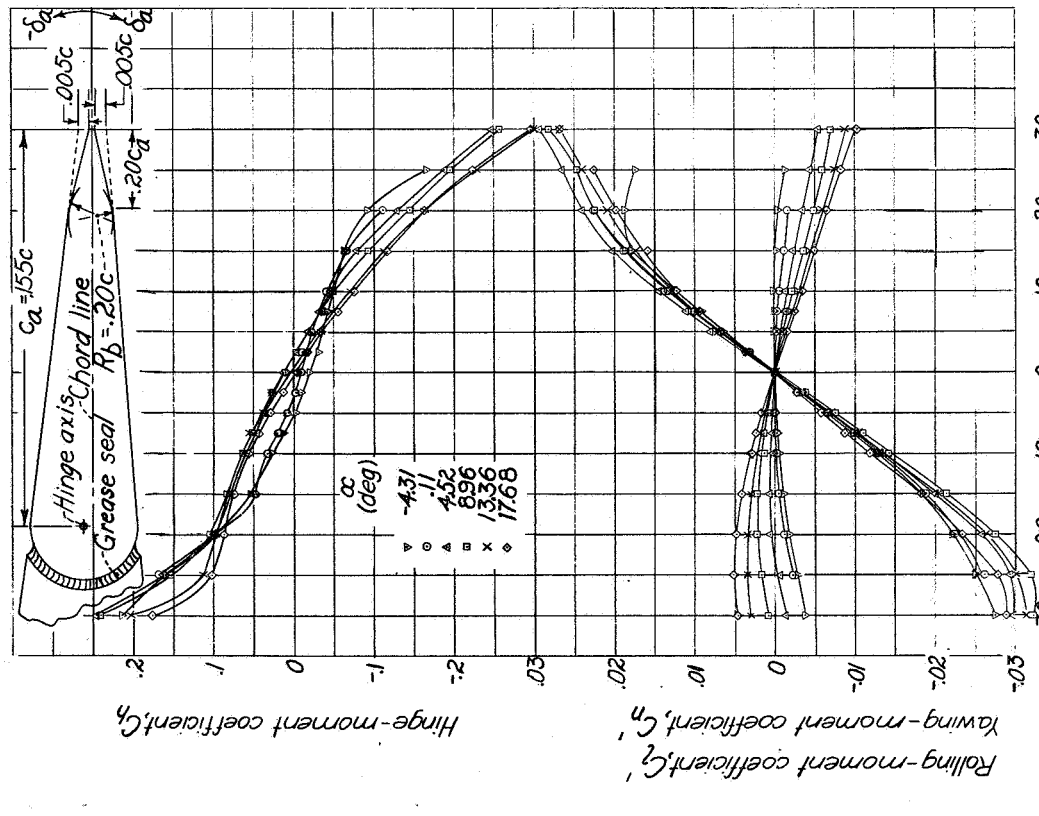

Figure 15.- Characteristics of a beveled aileron on the tapered-wing model. Sealed gap ; c_b, 0.20c_a ; Δt, 0.01c ; R_b, 0.20c.

L-228

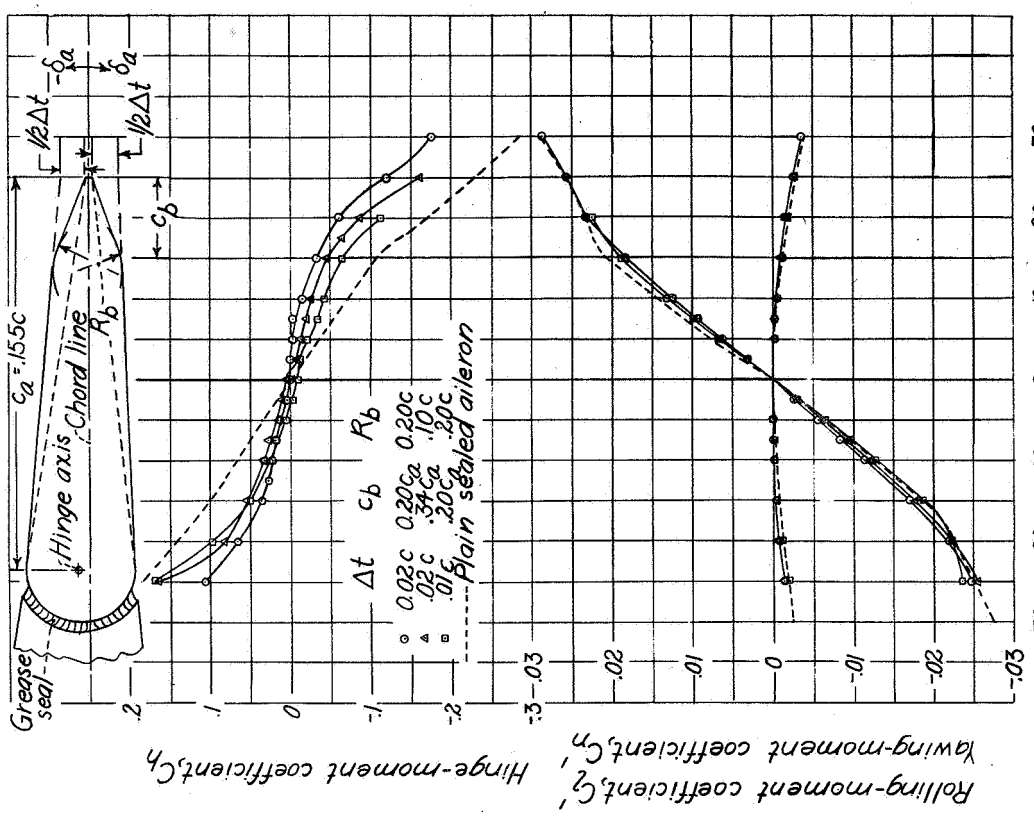

(b) Sealed gap ; rounded bevel corners.

Figure 17.- Concluded.

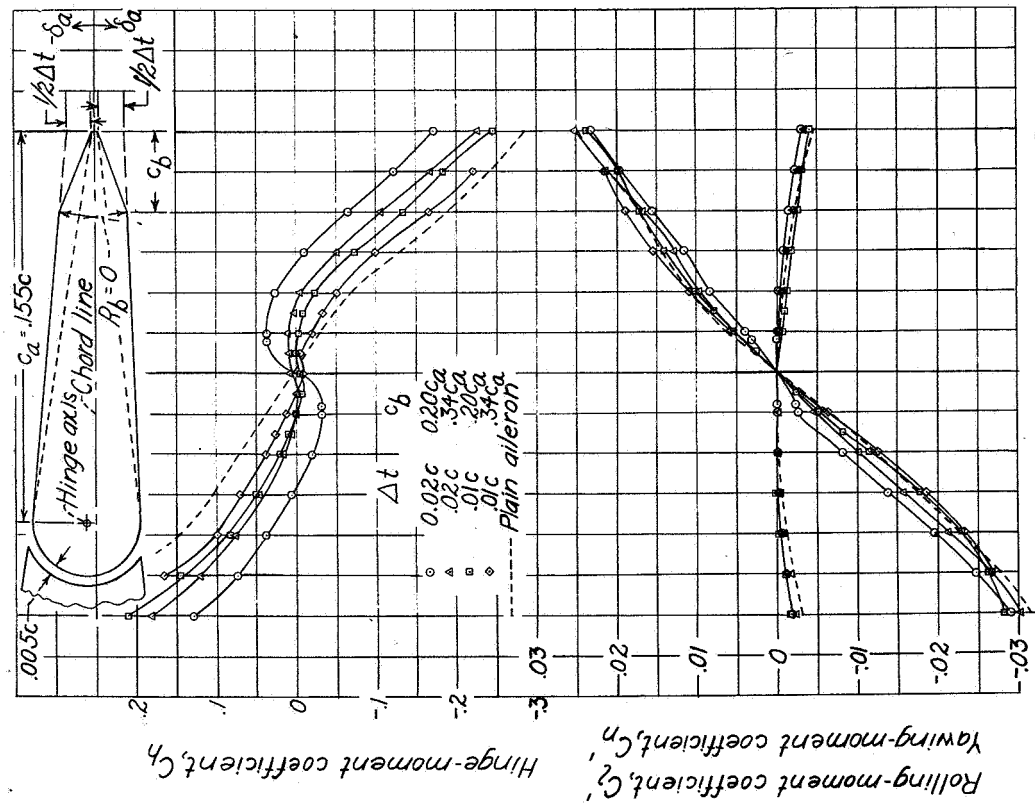

(a) 0.005c gap ; sharp bevel corners.

Figure 17 - Effect of bevel chord and thickness on the characteristics of beveled ailerons on the tapered-wing model. α, 0.11°.

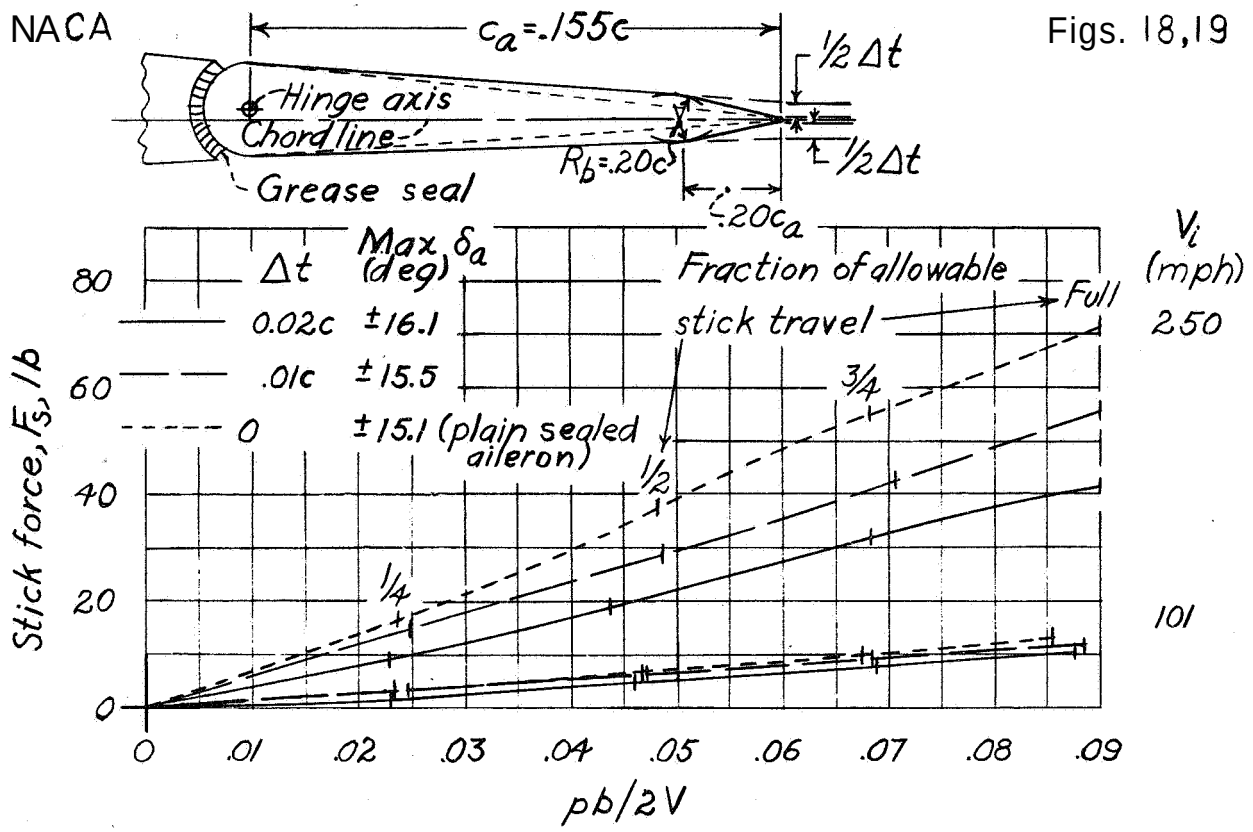

Figure 18.- Stick-force characteristics of the plain and beveled ailerons on the tapered wing. Sealed gap; c_b, 0.20c_a, R_b, 0.20c.

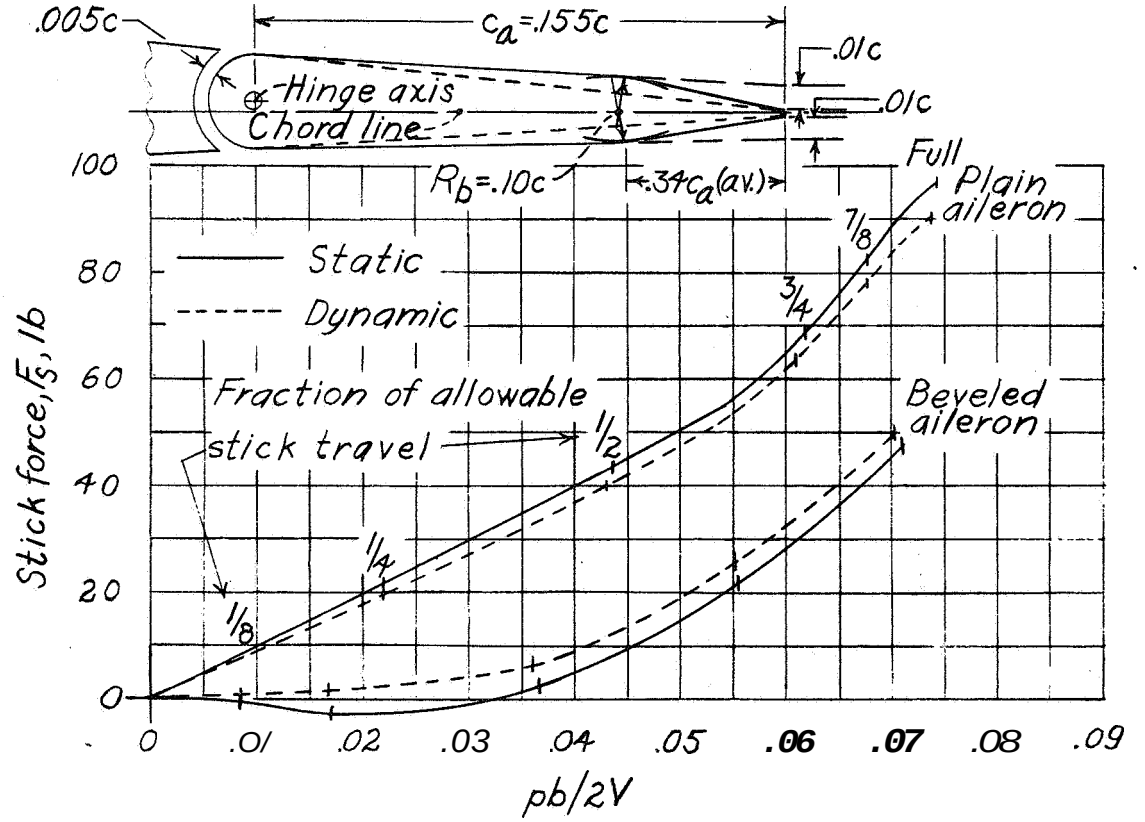

Figure 19.- Effect of rolling on the stick-force characteristics of plain and beveled ailerons on the tapered wing. 0.005c gap; maximum δ_a, ±16°; V_i > 250 miles per hour.